Published in final edited form as:
Am J Obstet Gynecol. 2008 April ; 198(4): 474.e1–474.11. doi:10.1016/j.ajog.2007.11.057.

Mechanical homeostasis is altered in uterine leiomyoma

Rebecca ROGERS, BS[a,b], **John NORIAN, MD**[b], **Mones ABU-ASAB, PhD**[c], **Gregory CHRISTMAN, MD**[d], **Minnie MALIK, PhD**[b], **Faye CHEN, PhD**[e], **Casey KORECKI**[f], **James IATRIDIS**[f], **William H. CATHERINO, MD, PhD**[b], **Rocky S TUAN**[e], **Phyllis LEPPERT, MD, PhD**[a,b], and **James H. SEGARS, MD**[a,b]

a *Reproductive Biology and Medicine Branch, NICHD, NIH, Bethesda, MD 20892*

b *Department of Obstetrics and Gynecology, Uniformed Services University of the Health Sciences, Bethesda, MD 20814*

c *Laboratory of Pathology, NCI, NIH, Bethesda, MD 20892*

d *Department of Obstetrics and Gynecology, University of Michigan, Ann Arbor, MI*

e *Cartilage Biology and Orthopaedics Branch, NIAMS, NIH, Bethesda, MD 20892*

f *School of Engineering, University of Vermont, Burlington, VT*

Abstract

Objective—Uterine leiomyoma produce an extracellular matrix (ECM) that is abnormal in its volume, content, and structure. Alterations in ECM can modify mechanical stress on cells, leading to activation of Rho-dependent signaling. Here we sought to determine whether the altered ECM produced by leiomyoma was accompanied by an altered state of mechanical homeostasis.

Study Design—Measurement of the mechanical response in paired leiomyoma and myometrium, immunogold, confocal microscopy, and immunohistochemical analyses.

Results—Leiomyoma were significantly stiffer than matched myometrium. The increased stiffness was associated with a moderate increase in total sulfated glycosaminoglycan content and a slight increase in hydroxyproline. Levels of the Rho-GEF, AKAP13, were increased and subcellular localization was altered in leiomyoma. Phosphorylation of p38MAPK was greater in leiomyoma extracts.

Conclusions—Leiomyoma cells are exposed to increased mechanical stress and show structural and biochemical features consistent with activation of solid-state signaling. The altered state of stress may contribute to growth of leiomyoma.

Keywords

Leiomyoma; mechanotransduction; solid state signaling; AKAP13; Brx; RhoA; fibroid

Corresponding author: James H. Segars, Building 10, CRC, 1E-3140, 10 Center Drive, NICHD, NIH, Bethesda, MD 20892, Phone: (301) 496-5800; Fax: (301)402-0884; e-mail: E-mail: segarsj@mail.nih.gov.

Presented in part at the: Annual Meeting of the American Society for Reproductive Medicine, Montreal Canada, October, 2005 and the American Gynecological and Obstetrical Society, Chicago, IL 2007

Condensation: Leiomyoma cells show structural and biochemical features consistent with activation of solid-state signaling. The altered state of mechanical stress may contribute to growth of these common tumors.

Introduction

Mechanical stress is a well-documented extracellular stimulus of muscle hypertrophy. The cellular process by which mechanical stress is converted to cell signaling is known as mechanotransduction or solid-state signaling (reviews1,2). Mechanical stresses imposed upon the extracellular matrix are transmitted through integrins,3 mechanotransducers, and caveoli4 to biochemical signals in the cell. Downstream cellular signaling pathways of mechanotransduction include mitogen-activated protein kinases (MAPK), phosphatidylinositol-3 kinase/Akt, Janus kinase/signal transducer,5 and nitric oxide.6 Rho family small GTPases play a critical role in the process. Rho-GTPases function as molecular switches that are on in the GTP-bound state and off in the GDP-bound state.7 Rho family members influence cytoskeletal rearrangement, contractility, cell migration and cell proliferation.8 While the fundamental elements of the pathway have been elucidated in other cell types, such as cardiomyocytes, the precise molecular mechanisms that transduce mechanical signals in uterine muscle cells remain incompletely defined.

In addition to physiologic activation, pathologically altered states of mechanical stress can cause fibrosis by stimulating fibroblasts to deposit excessive extracellular matrix.9 Little is known about the pathologic response of uterine smooth muscle cells to mechanical stress, in particular whether altered mechanical stress might lead to fibroblast transformation and deposition of excessive extracellular matrix (ECM), for example as a uterine fibroid. One key feature of uterine fibroids is the production of excessive amounts of extracellular matrix.10 In fact, growth of large fibroids (greater than 5 cm) was largely due to deposition of ECM11 and the composition of this excessive ECM differed from smaller fibroids and myometrium.12, 13 Prior studies of ECM in fibroids have reported increased levels of total glycosaminoglycans (GAGs) and a reduction in hylauronic acid.12–16 Several groups have reported the extracellular matrix in leiomyoma is altered in both content 12,15,17 and structure.15,18 Because collagen provides structural support to the ECM, the random orientation of collagen fibrils in leiomyoma18 suggests that the mechanical properties of leiomyoma may differ from normal uterine tissue.

In addition to influencing fibrosis, accumulating evidence indicates that altered mechanical stress plays an important role in cell growth and tumorogenesis.19 Many tumors have been shown to have an elevated elastic modulus or stiffness 20, an attribute used clinically to detect metastatic nodules on peritoneal surfaces at laparotomy and with imaging modalities.21 Specifically, Rho-GTPases were elevated in stiff tumors22 and activation of the Rho-dependent kinase, ROCK, has been shown to cause tumor cell dissemination.23 Activation of Rho-dependent cytoskeletal tension led to increased levels of ERK and cell proliferation24 and was a requisite step in acquisition of a malignant phenotype of breast cancers.19

The two cardinal features of uterine fibroids, excessive fibrosis and tumor formation, suggest that fibroblasts within a leiomyoma may be exposed to increased mechanical stress. To determine whether altered mechanical stress may play a role in fibroid development we characterized the state of mechanical homeostasis in matched surgical specimens of leiomyoma and normal myometrium. The findings suggested that the production of an abnormal ECM in fibroids was accompanied by a state of altered homeostasis in leiomyoma. Improved understanding of the mechanical response of uterine muscle cells may contribute to understanding of both pathologic and physiologic states of uterine smooth muscle.

Materials and Methods

Tissue Collection

Tissues were collected from women undergoing hysterectomy for symptomatic leiomyoma in IRB-approved studies at the National Naval Medical Center and the NIH. For western blots, tissue was snap-frozen on dry ice and stored at −70°C until processed. For immunohistochemistry, samples were frozen in cryoprotectant (OCT 4583, Tissue-Tek, Elkhart, IN) or formalin-fixed and embedded in paraffin. For immunogold studies tissue was fixed in formalin. Characteristics of patients and leiomyoma studied are summarized in Table I.

Mechanical Testing

From fresh or snap-frozen leiomyoma tissues, 4–5 mm. cylindrical pieces were cut using an 8mm biopsy punch (Miltex, Tuttlingen, Germany) and a microtome blade. Height and diameter were recorded and tissue was subjected to a mechanical testing protocol using displacement control.25 Young's modulus is defined as the longitudinal deformation in terms of strain (fractional change in length) in response to longitudinal stress (force per unit area). Because most tissues exhibit non-linear viscoelastic changes in physiological ranges of stress, we used equilibrium assessment of Young's moduli.

GAG Assay

Small pieces of frozen fibroid and myometrium specimens were weighed and digested overnight in digestion buffer (0.1M NaAc, 10mM Cystein HCl, 50mM EDTA, plus 20uL papain/ml buffer). GAG concentration of completely digested samples was determined using the Blyscan Sulfated Glycosaminoglycan Assay (Biocolor, Newtownabbey, UK) per manufacturer's instructions. Hydroxyproline content of each sample was determined after Proteinase-K digestion as described.25

FITC phalloidin stain

Snap-frozen tissue blocks were cut into 5 μm sections onto glass slides, fixed for 15 mins. in 3.7% paraformaldehyde, were washed 3 × 5 mins. in PBS, permeabilized in 0.2% Triton X-100 in PBS for 1hr., washed in PBS with 0.05% Triton, and blocked in 1% BSA in PBS for 1 hr. Slides were then placed in a dark humidity chamber for 1hr. in 5ug/ml FITC Phalloidin (Sigma-Aldrich, St. Louis, MO). After rinses in PBS/0.05% Triton, slides were mounted in media with DAPI (Vector Laboratories, Burlingame, CA), cover-slipped and visualized.

Western blots

Protein was isolated according to a previously described protocol.27 Samples (50μg) were resolved in Tris-Glycine gels (Invitrogen) and transferred to Hybond nitrocellulose membranes (Amersham, Piscataway, NJ). Membranes were blocked for 2–3 hours at 4°C in TBS with 0.05% Tween-20 (TBST) and 5.0% evaporated milk and incubated overnight at 4°C in TBST with 0.1% BSA and primary antibodies. Membranes were rinsed 3 times in TBST for 5 minutes between all incubations. Secondary antibody was added in TBST with 0.1%BSA at room temperature for 1 hr. Supersignal developing reagents were used according to the directions (Pierce, Rockford, IL) and membranes were exposed to film. For each antibody used, HRP-conjugated B-actin (Santacruz Biotechnologies, Santa Cruz, CA) was used to confirm equal protein loading. Cos-7 lysates transfected with a 170kDa form of AKAP13 (Brx) was used as a positive control. Recombinant RhoA (Calbiochem) was used as a control. Anti-phosphorylated p38MAPK (SC 7973, Santa Cruz, CA) was purchased.

Microarray

Sample collection, microarray analysis were previously described.17,28 The existing database was queried for genes known to be involved in mechanotransduction. Results were from 5 paired myometrial and fibroid samples.

Immunohistochemistry (IHC)

Paraffin-embedded tissue samples were cut into 5 micron sections. Sections were stained according to the Vectastain Elite ABC kit protocol (Vector Laboratories) as previously described28 with the following modifications. Antigen retrieval was performed by boiling water and unmasking solution in a pressure cooker. Slides were incubated in primary antibody either for 3 hours at room temperature or 4°C overnight. All subsequent steps were carried out according to the manufacturer's instructions (Vector Laboratories). Sections with no primary or no secondary antibodies served as controls.

Immunogold

Tissue pieces were removed from a paraffin block and deparaffinated in xylene or taken directly from formalin and placed in absolute ethanol and embedded in LR White (SPI, West Chester, PA). Ultrathin sections were mounted on 150-mesh uncoated nickel grids. Sections were hydrated in blocking buffer (BB=PBS, 0.1% Tween-20, 0.5% cold-water fish gelatin [Ted Pella, Inc., Redding, CA]) for 20 minutes, then incubated in buffer containing AKAP13 primary antibody (1:125) for an hour. Samples not incubated in primary antibody served as a control. Samples were placed in BB with 2% goat serum for 5 min., washed twice in BB without serum for 2 min., incubated in 10nm gold-conjugated secondary antibody (1:1000) (Ted Pella Inc, Redding, CA) for 1 hr, and were washed 2 times in PBS and twice in deionized water. Dried grids were stained with uranyl acetate for 3 min., rinsed 3 times and allowed to dry again.

Confocal microscopy

Cells were grown on glass chamber slides (Nalge Nunc Int., Rochester, NY), fixed with cold methanol and permeabilized with 0.2% Triton-X 100 (Sigma-Aldrich, St. Louis, MO). Non-specific sites were blocked using 1% BSA and 10% normal goat serum and slides were incubated either with antibody to alpha smooth muscle actin and 2665 affinity-purified anti-Brx (AKAP13) polyclonal antibody29 at 1:50 dilution overnight at 4°C. For secondary antibody either FITC (anti-rabbit, 1:100) or Alexa-594 (anti-mouse, 1μg/ml; Invitrogen) was used. DAPI (Sigma-Aldrich, St. Louis, MO) was added at 0.1μg/ml in PBS before the cells were examined with an Axiovert 405M epifluorescence inverted light microscope (Carl Zeiss, Oberkochen, Germany). Images were acquired with a CCD camera (Hamamatsu Orca, Shizuoka, Japan).

Results

The Young's modulus was quantified with average values of 4.9kPa and 18.6kPa for myometrial and leiomyoma samples, respectively (Fig 1). Variation was noted between specimens and within specimens, but uterine leiomyoma tissues were typically 2–3 fold stiffer than matched myometrium ($P<0.05$). Since the presence of an excessive mechanical load can influence extracellular matrix formation, we measured sulfated glycosaminoglycans and hydroxyproline content in a subset of samples exposed to testing. Total sulfated glycosaminoglycan content per wet weight of tissue was increased in leiomyoma compared to matched myometrium. Hydroxyproline content was also increased in leiomyoma compared to matched myometrium samples. These two findings are consistent with prior reported levels of glycosaminoglycan content in leiomyoma 12–14, and suggest that both amount of GAGs and increased collagen may contribute to the stiffness observed in fibroid tumors.

Cells exposed to increased mechanical loading may exhibit structural changes and altered expression of structural support proteins, such as actin; therefore, we examined smooth muscle alpha actin and F-actin in matched surgical specimens of leiomyoma and myometrium. Phalloidin staining revealed a striking difference between leiomyoma and myometrial tissues, consistent with our observation of disordered ECM in leiomyoma (Fig. 2). Cell shape in leiomyoma was angular with a compressed appearance in comparison to myometrium. These findings are consistent with the finding that tissue stiffness was increased in leiomyoma compared to myometrium.

The finding of increased stiffness led to the question: did leiomyoma exhibit biochemical evidence of activation of solid state signaling? To characterize the levels of factors known to be involved in mechanotransduction, we queried our cDNA microarray data of 33,000 transcripts.17,28 As shown in Table II, several factors involved in solid state signaling were differentially expressed in leiomyoma. Transcripts of one protein, AKAP13 a Rho-GEF, were over expressed 4 fold based on microarray results. We decided to focus on this factor because: 1) RhoA is a known target of AKAP13 30 and RhoA is involved in the cellular response to mechanical stress 8,19,22–24; 2) it was the only Rho-GEF differentially expressed based on the microarray results; and 3) we had cloned this factor based upon its ability to augment estrogen action 29,31 and leiomyoma are known to be estrogen-responsive.

To confirm the array data, we performed western analyses on paired fibroid and myometrial samples. Western analysis using antisera directed against AKAP13 revealed a 220kDa band in fibroid of the expected molecular weight (Fig. 3). Since AKAP13 is differentially spliced, we confirmed identification of the 220kDa using a monoclonal antibody to AKAP13. Both antibodies detected a 220kDa band. Quantification of western results revealed AKAP13 was over expressed in the majority of fibroids, in support of the microarray (mRNA) results. Levels of non-membrane associated RhoA have been noted to correlate with activation of RhoA.4 We performed immunohistochemical staining for Rho in matched fibroid and myometrial samples to determine whether increases in AKAP13 were coupled with increased levels of RhoA. While some leiomyoma did have greater levels of RhoA, no consistent pattern emerged (Fig. 3D).

Since mechanical homeostasis appeared to be altered based on direct measurement of tissue, and the Rho-GEF AKAP13 was elevated in most, but not all samples, we questioned whether the subcellular localization of AKAP13 might be altered in leiomyoma relative to myometrium. To examine the subcellular localization in native tissues we performed immunohistochemical analysis of matched fibroid and myometrial samples (Fig. 4). These studies suggested that the subcellular localization of AKAP13 was altered in fibroids, with increased staining often near the cell membrane or nuclear envelope, but resolution was not sufficient to accurately define the subcellular localization. To more precisely identify the subcellular localization of AKAP13 in uterine fibroids we performed immunogold studies. Electron microscopy substantiated the increased localization of AKAP13 in perinuclear region and further suggested that the protein may associate with filaments in the cytoplasm.

Because AKAP13 has been shown to regulate actin filament nucleation, the possible association with cytoskeletal filaments suggested that AKAP13 might function through a direct association with the actin cytoskeleton. To examine this possibility, we performed confocal microscopy on immortalized uterine fibroid and myometrial cells (Fig. 5). These cells have been characterized and closely resemble native leiomyoma and myometrium.32 In cells derived from leiomyoma, the staining for AKAP13 was robustly present and localized primarily to cytofilaments in comparison with cells derived from myometrium. These observations suggest that the subcellular distribution of AKAP13 is altered in leiomyoma.

We reasoned that if steady-state levels of AKAP13 protein were increased in most uterine leiomyoma, downstream targets may be activated. Two known targets of AKAP13 are RhoA and p38MAPK. We were unable to consistently measure active Rho in lysates prepared from surgical samples (e.g., rhotekin assays). However, we prepared rapid protein lysates from three leiomyoma and myometrial samples and assayed for the phosphorylated form of p38MAPK using immunoblot and immunhistochemical staining. The results indicated that levels of phospho-p38MAPK were increased in uterine leiomyoma compared to matched myometrial samples.

Comment

The findings suggest that cells comprising uterine leiomyoma are exposed to increased mechanical stress and exhibit downstream findings consistent with activation of solid-state signaling. Consistent with the increased physical force, cells in leiomyomata exhibited structural changes associated with mechanical stress, such as altered actin organization, altered collagen fibers, an angular shape and distortion of the nuclear envelope. The response of leiomyoma cells to the increased mechanical loading was production of a disordered and excessive ECM.

Activated states of solid-state signaling have been shown to affect cell growth. Proliferation of breast cancer cells was significantly increased when the tension reached 1.2kPa. However, breast cells with chromosomal anomalies consistent with metastasis did not metastasize until mechanical force was greater than 5kPa.19 Breast tumors exhibited an average elastic modulus of 4.0kPa, but can differ from surrounding tissue by 90 fold.21 Myometrium stiffness averaged 5kPa, while fibroid tumors from the same uterus typically exhibited a 3 fold increase in stiffness. The 3 fold increase in stiffness observed relative to surrounding muscle may be sufficient to increase proliferation, or reduce apoptosis of the leiomyoma cells.

The results suggest that leiomyoma cells exhibit abnormal sensing of mechanical stress. It is reasonable to assume the cells themselves have a tensile elastic modulus approximately 0.52kPa33 (the value for chondrocytes). In contrast, normal myometrium had an elastic modulus of 5kPa, indicating that 90% of the stiffness of myometrium could be attributed to structural aspects of the tissue. For leiomyoma, 97% of the measured stiffness would be attributable to structure of the ECM if the cell modulus was similar to chondrocytes. The increased tissue stiffness may suggest that leiomyoma cells do not properly sense applied mechanical stress (have in appropriately low signaling) and as a result produce excessive ECM. An alternative possibility is leiomyoma cells produce excessive amounts of load-bearing ECM to ‘stress-shield’ themselves (cells are overly sensitive to mechanical stress). In either scenario, mechanical sensing by leiomyoma cells appears to be abnormal.

Any physical measurement of tissues is limited by the fact that physiologic tissues are non-homogenous in viscoelastic properties and anisotropic. Although we are not aware of any prior mechanical assessment in uterine muscle, skeletal muscle was softer along fibers than across fibers.21 Nonetheless the 3 fold difference observed was greater than differences attributable to specimen orientation alone. To address the question of ECM content, we measured GAGs and collagen structure in the same samples that were subjected to mechanical testing. The changes in GAGs and collagen were consistent with prior reports.12–16

Our previous studies of uterine fibroids using microarrays have served to focus attention on the ECM of uterine fibroids and the similarity of fibroids to tissue remodeling and repair.34 We noted that fibroids were composed of an ECM with altered organization of structural elements, such as collagen fibers.18 In addition, we17 and others12,15,35 have noted that fibroid express altered levels of key proteoglycans, such as dermatopontin and versican. The

current study supports and extends upon the notion of altered tissue repair, because formation of a load-bearing ECM is a key step in tissue repair. It is worth noting that excessive mechanical stress of muscle cells and abnormal repair has been shown to induce fibrosis in other muscular tissues, for example in the heart.36

We were somewhat surprised that microarray results revealed increased levels of the Rho-GEF, AKAP13 (a.k.a. Brx) because our prior studies of AKAP13 had focused on its ability to augment estrogen 29,31 and glucocorticoid action.37 We were intrigued by the fact that sex steroids influence leiomyoma growth, but conversely excessive glucocorticoids (such as Cushing's Sydrome) cause muscle atrophy. Since the microarray results singled out this transcript, we proceeded to characterize expression of AKAP13 in leiomyoma. Altered expression of AKAP13 in leiomyoma was supported by western analysis, immunohistochemical stains, confocal microscopy and immunogold studies. Consistent with an important role of AKAP13 in muscle differentiation, targeted deletion of AKAP13 in the mouse resulted in an embryonic lethal phenotype due to failure of cardiomyocyte differentiation and cardiac rupture in utero.38

We found that in muscle cells AKAP13 was associated with cytoskeletal structures, whereas in ovarian tumors 39 we did not detect a similar subcellular pattern of localization. Our interpretation of these seemingly conflicting results is that the *AKAP13* gene is differentially-spliced and targeting of different splice variants to distinct subcellular compartments may be dictated by regions present in some transcripts, but lacking in others. We are currently examining this possibility. At present, the precise molecular coupling of AKAP13 to cytoskeletal proteins is unclear, but splice variants of AKAP13 has been shown to bind filamin 40 and filamins interact with caveole 41,42, which are known to respond to mechanical force. 4 In addition, AKAP13 variants bind alpha-catulin30 and alpha catulin interacts with catenins and cadherins. Collectively, these observations suggest an indirect molecular link might couple AKAP13 to the mechanical sensing protein complexes.

In summary, these results are consistent with activation of cellular tension in leiomyoma. The results are in agreement with the general understanding that TGF-beta signaling is augmented in leiomyoma leading to secretion of excessive amounts of ECM. These observations indicate that cells within a leiomyoma exist in a state of altered mechanical homeostasis which likely contributes to production of excessive amounts of ECM as well as proliferation and reduced levels of apoptosis.

Acknowledgments

The authors wish to recognize critical assistance and instruction by Drs. Paul Driggers and Lars Rackwitz. Support by Drs. George Chrousos and Alan DeCherney was critical for completion of the project. Joy provided technical assistance. Julia Sampson was supported by the Howard Hughes Foundation. This research was supported by the NIH intramural program of the Reproductive Biology and Medicine Branch, HD-Z01-008737-URE.

Financial support: This research was supported by the intramural research programs of NCI and NICHD; ZO1-HD-008737-03 URE.

References

1. Huang S, Ingber DE. Cell tension, matrix mechanics, and cancer development. Cancer Cell 2005;8:175–76. [PubMed: 16169461]
2. Alenghat FJ, Ingber DE. Mechanotransduction: all signals point to cytoskeleton, matrix and integrins. Sci STKE 2002;119:Pe6. [PubMed: 11842240]
3. Geiger B, Bershadsky A. Exploring the neighborhood: adhesion-coupled cell mechanosensors. Cell 2002;110:139–142. [PubMed: 12150922]

4. Kawamura S, Miyamoto S, Brown JH. Initiation and transduction of stretch-induced RhoA and Rac1 activation through caveolae. J Biol Chem 2003;278:31111–7. [PubMed: 12777392]
5. Ruwhof C, van der Laarse A. Mechanical stress-induced cardiac hypertrophy: mechanisms and signal transduction pathways. Cardiovascular Res 2000;47:223–37.
6. Petroff MGV, Kim SH, Pepe S, Dessy C, Marban E, Balligand J-L, et al. Endogenous nitric oxide mechanisms mediate the stretch dependence of Ca+2 release in cardiomyocytes. Nat Cell Biol 2001;3:867–73. [PubMed: 11584267]
7. Schmidt A, Hall A. Guanine nucleotide exchange factors for the Rho GTPases: turning on the switch. Genes & Dev 2002;16:1587–1609. [PubMed: 12101119]
8. Wettschureck N, Offermanns S. Rho/Rho-kinase mediated signaling in physiology and pathophysiology. J Mol Med 2002;80:629–638. [PubMed: 12395147]
9. Paszek MJ, Weaver VM. The tension mounts: mechanics meets morphogenesis and malignancy. J Mam Gland Biol Neopl 2004;9:325–342.
10. Walker CL, Stewart EA. Uterine fibroids: the elephant in the room. Science 2005;308:1589–1592. [PubMed: 15947177]
11. Davis, BJ. The NIEHS Uterine Fibroid Study: preliminary results. Presented at: Advances in Leiomyoma Research: 2nd NIH International Congress; Bethesda, MD. February 24–25; 2005.
12. Wolanska M, Sobolewski K, Drozdzewicz M, Bankowski E. Extracellular matrix components in uterine leiomyoma and their alteration during the tumour growth. Mol Cell Biochem 1998;189:145–52. [PubMed: 9879665]
13. Mitropoulou TN, Theocharis AD, Stagiannis KD, Karamanos NK. Identification, quantification and fine structural characterization of glycosaminoglycans from uterine leiomyoma and normal myometrium. Biochimie 2001;83:529–536. [PubMed: 11506898]
14. Hjelm A, Ekman-Ordeberg G, Barchan K, Malmstrom A. Identification of the major proteoglycans from human myometrium. Acta Obstet Gynecol Scand 2001;80:1084–1090. [PubMed: 11846703]
15. Berto AGA, Sampaio LO, Franco CRC, Cesar RM, Michelacci YM. A comparative analysis of structure and spatial distribution of decorin in human leiomyoma and normal myometrium. Biochim Biophys Acta 2003;1619:98–112. [PubMed: 12495820]
16. Rein MS, Barbieri RL, Welch W, Gleason RE, Caulfield JP, Friedman AJ. The concentrations of collagen-associated amino acids are higher in GnRH agonist-treated uterine myomas. Obstet Gynecol 1993;82:901–5. [PubMed: 8233262]
17. Catherino WH, Leppert PC, Stenmark MH, Payson M, Potlog-Nahari C, Nieman LK, et al. Reduced dermatopontin expression is a molecular link between uterine leiomyomas and keloids. Genes Chromosomes Cancer 2004;40:204–17. [PubMed: 15139000]
18. Leppert PC, Baginski T, Prupas C, Catherino W, Pletcher S, Segars JH. Comparative ultrastructure of collagen fibrils in uterine leiomyomas and normal myometrium. Fertil Steril 2004;82:1182–1187. [PubMed: 15474093]
19. Paszek MJ, Zahir N, Johnson KR, Lakins JN, Rozenberg GI, Gefen A, et al. Tensional homeostasis and the malignant phenotype. Cancer Cell 2005;8:241–54. [PubMed: 16169468]
20. Beil M, Micoulet A, von Wichert G, Paschke S, Walther P, Omary MB, et al. Sphingosylphosphorylcholine regulates keratin network architecture and visco-elastic properties of human cancer cells. Nat Cell Biol 2003;5:803–11. [PubMed: 12942086]
21. Greenleaf JF, Fatemi M, Insana M. Selected methods for imaging elastic properties of biological tissues. Annu Rev Biomed Eng 2003;5:57–78. [PubMed: 12704084]
22. Fritz G, Just I, Kaina Bernd. Rho GTPases are over-expressed in human tumors. Int J Cancer 1999;81:682–87. [PubMed: 10328216]
23. Croft DR, Sahai E, Mavria G, Li S, Tsai J, Lee WMF, et al. Conditional ROCK activation in vivo induces tumor cell dissemination and angiogenesis. Cancer Res 2004;64:8994–9001. [PubMed: 15604264]
24. Wang F, Weaver VM, Petersen OL, Larabell CA, Dedhar S, Briand P, et al. Recipocal interactions between β1-integrin and epidermal growth factor receptor in three-dimensional basement membrane cultures: a different perspective in epithelial biology. Proc Natl Acad Sci USA 1998;95:14821–14826. [PubMed: 9843973]

25. Mauck RL, Soltz MA, Wang CC, Wong DD, Chao PH, Valhmu WB, et al. Functional tissue engineering of articular cartilage through dynamic loading of chondrocyte-seeded agarose gels. J Biomech Eng 2000;122:252–60. [PubMed: 10923293]
26. Reddy GK, Enwemeka CS. A simplified method for the analysis of hydroxyproline in biologic tissues. Clin Biochem 1996;29:225–229. [PubMed: 8740508]
27. Tsibris JCM, Porter KB, Jazayeri A, Tzimas G, Nau H, Huang H, et al. Human uterine leiomyoma express higher levels of peroxisome proliferator–activated receptor γ, retinoid receptor α and all-trans retinoic acid than myometrium. Cancer Res 1999;59:5737–5744. [PubMed: 10582693]
28. Catherino WH, Prupas C, Tsibris JCM, Leppert PC, Payson M, Nieman L, et al. Strategy for elucidating differentially expressed genes in leiomyomata identified by microarray. Fertil Steril 2003;80:282–90. [PubMed: 12909487]
29. Rubino D, Driggers P, Arbit D, Kemp L, Miller B, Coso O, et al. Characterization of Brx, a novel DBL family member that modulates estrogen action. Oncogene 1998;16:2513–2526. [PubMed: 9627117]
30. Park B, Nguyen N, Dutt P, Merdek KD, Bashar M, Sterpetti P, et al. Association of Lbc Rho guanine nucleotide exchange factor with α-catenin-related protein, α-catulin/CTNNAL1, supports serum response factor activation. J Biol Chem 2002;277:45361–45370. [PubMed: 12270917]
31. Driggers PH, Segars JH, Rubino DM. The proto-oncoprotein Brx activates estrogen receptor β by a p38 mitogen-activated protein kinase pathway. J Biol Chem 2001;276:46792–476797. [PubMed: 11579095]
32. Malik M, Catherino WH. Novel method to characterize primary cultures of leiomyoma and myometrium with the use of confirmatory biomarker gene arrays. Fertil Steril. 2007in press
33. Iatridis JC, Wu J, Yandow JA, Langevin HM. Subcutaneous tissue mechanical behavior is linear and viscoelastic under uniaxial tension. Connect Tissue Res 2003;44:208–217. [PubMed: 14660091]
34. Leppert PC, Catherino WH, Segars JH. A new hypothesis about the origin of uterine fibroids based on gene expression profiling with microarrays. Am J Obstet Gynecol 2006;195:415–20. [PubMed: 16635466]
35. Chegini N, Verala J, Luo X, Williams RS. Gene expression profile of leiomyoma and myometrium and the effect of gonadotropin releasing hormone analogue therapy. J Soc Gynecol Investig 2003;10:161–71.
36. Sano M, Minamino T, Toko H, Miyauchi H, Orimo M, Qin Y, et al. p53-induced inhibition of Hif-1 causes cardiac dysfunction during pressure overload. Nature 2007;446:444–8. [PubMed: 17334357]
37. Kino T, Souvatzoglou E, Charmandari E, Ichijo T, Driggers P, Mayers C, et al. Rho family guanine nucleotide exchange factor Brx couples extracellular signals to the glucocorticoid signaling system. J Biol Chem 2006;281:9118–9126. [PubMed: 16469733]
38. Mayers CM, Wadell J, McLean K, Venere M, Sarber K, Malik M, et al. The Rho-GEF AKAP13 (Brx) is essential for cardiac development and sarcomere integrity in mice. Submitted
39. Miller BT, Rubino DM, Driggers PH, Haddad B, Cisar M, Gray K, et al. Expression of brx proto-oncogene in normal ovary and in epithelial ovarian neoplasms. Am J Obstet Gynecol 2000;182:286–295. [PubMed: 10694326]
40. Pi M, Spurney RF, Tu Q, Hinson T, Quarles LD. Calcium-sensing receptor activation of Rho involves filamin and Rho-guanine nucleotide exchange factor. Endocrinology 2002;143:3830–3838. [PubMed: 12239094]
41. Stahlhut M, van Deurs B. Identification of filamin as a novel ligand for caveolin-1: evidence for the organization of caveolin-1-associated membrane domains by the actin cytoskeleton. Mol Biol Cell 2000;11:325–337. [PubMed: 10637311]
42. Vadlamundi RK, Li F, Adam L, Nguyen D, Ohta Y, Stossel TP, et al. Filamin is essential in actin cytoskeletal assembly mediated by p21-activated kinase 1. Nature Cell Biol 2002;4:681–90. [PubMed: 12198493]

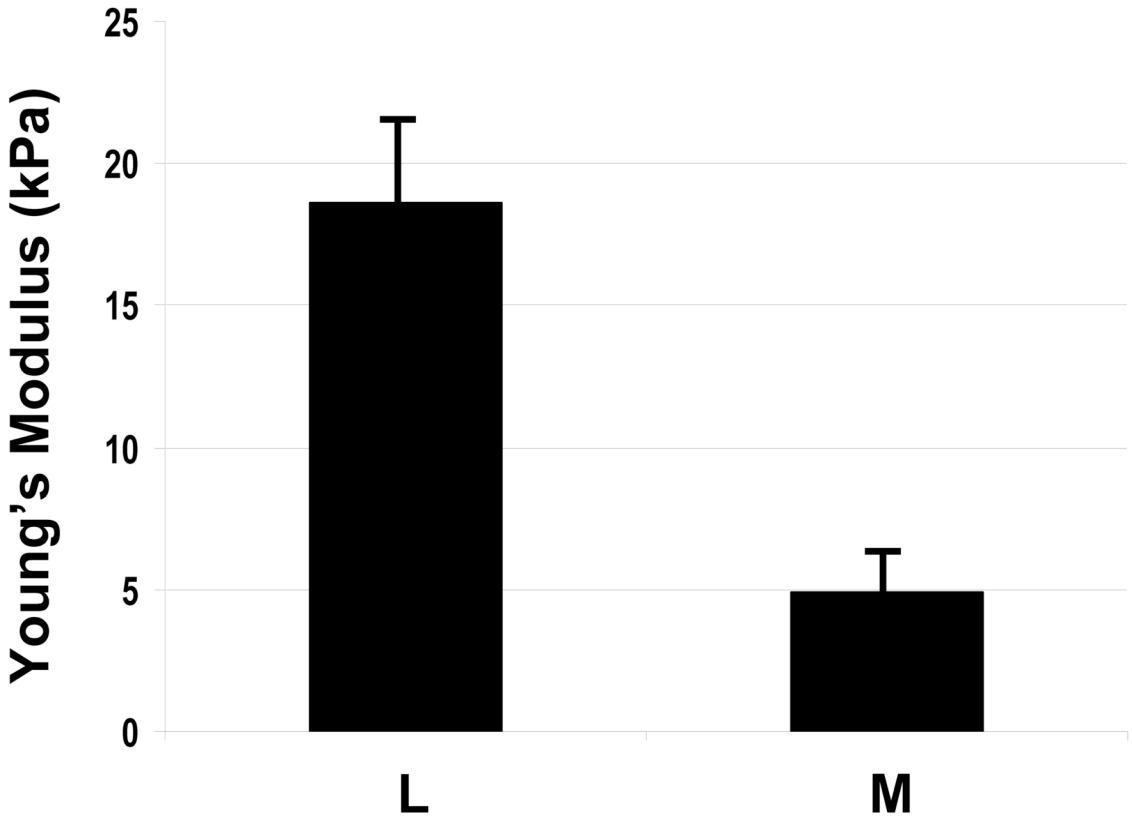

Figure 1B

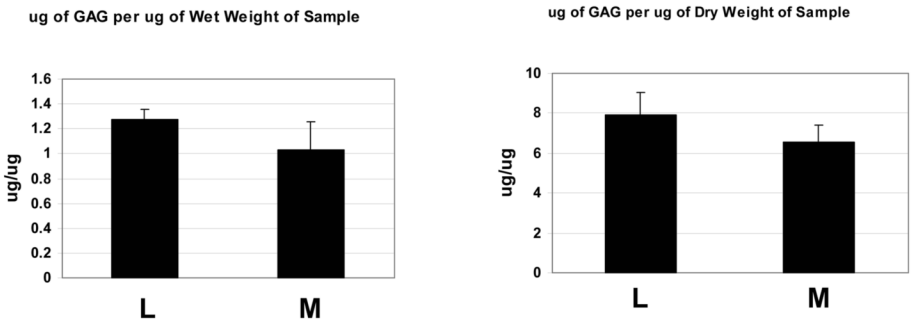

Figure 1C

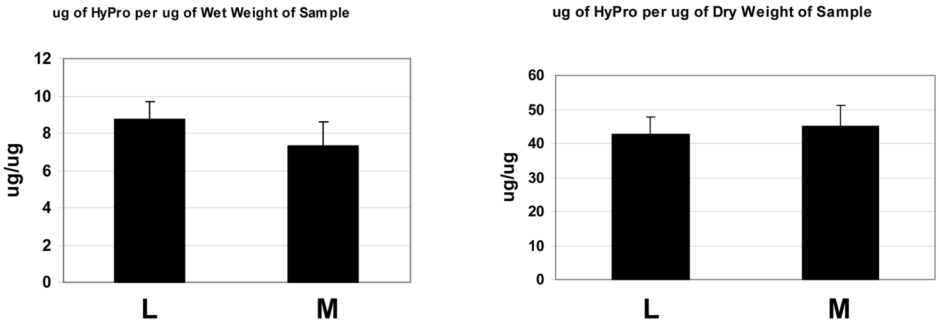

Figure 1. Mechanical testing in matched surgical specimens of uterine leiomyoma and myometrium

1A: Measurement of compressive resistance to 10% strain (Young's modulus) in leiomyoma and myometrial samples. Y=kilopascals (kPa), mean±SEM. X=samples of myometrium (M) or leiomyoma (L). Results were replicated in four independent studies.

1B: Measurement of total sulfated GAG content in matched leiomyoma and myometrial samples analyzed by compression using the blyscan method for wet (left panel) and dry weight (right panel). Y axes= micrograms of GAG per microgram of sample. X axes=sample myometrium (M) or leiomyoma (L). Results shown are averages of 3 representative assays.

1D: Hydroxyproline measurement in matched leiomyoma (L) and myometrial (M) samples corrected for wet and dry weight, as shown. Results shown are representative of 3 assays.

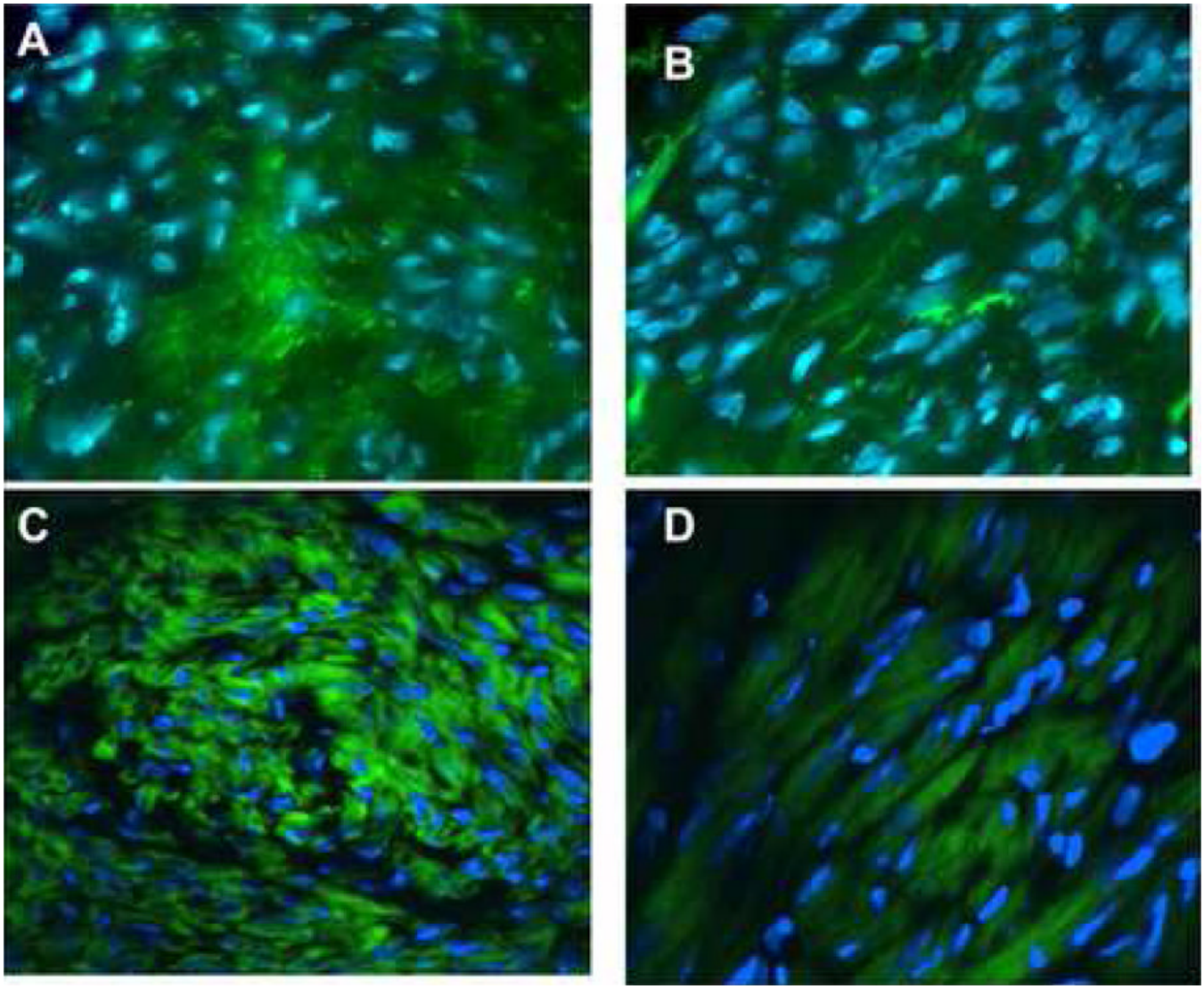

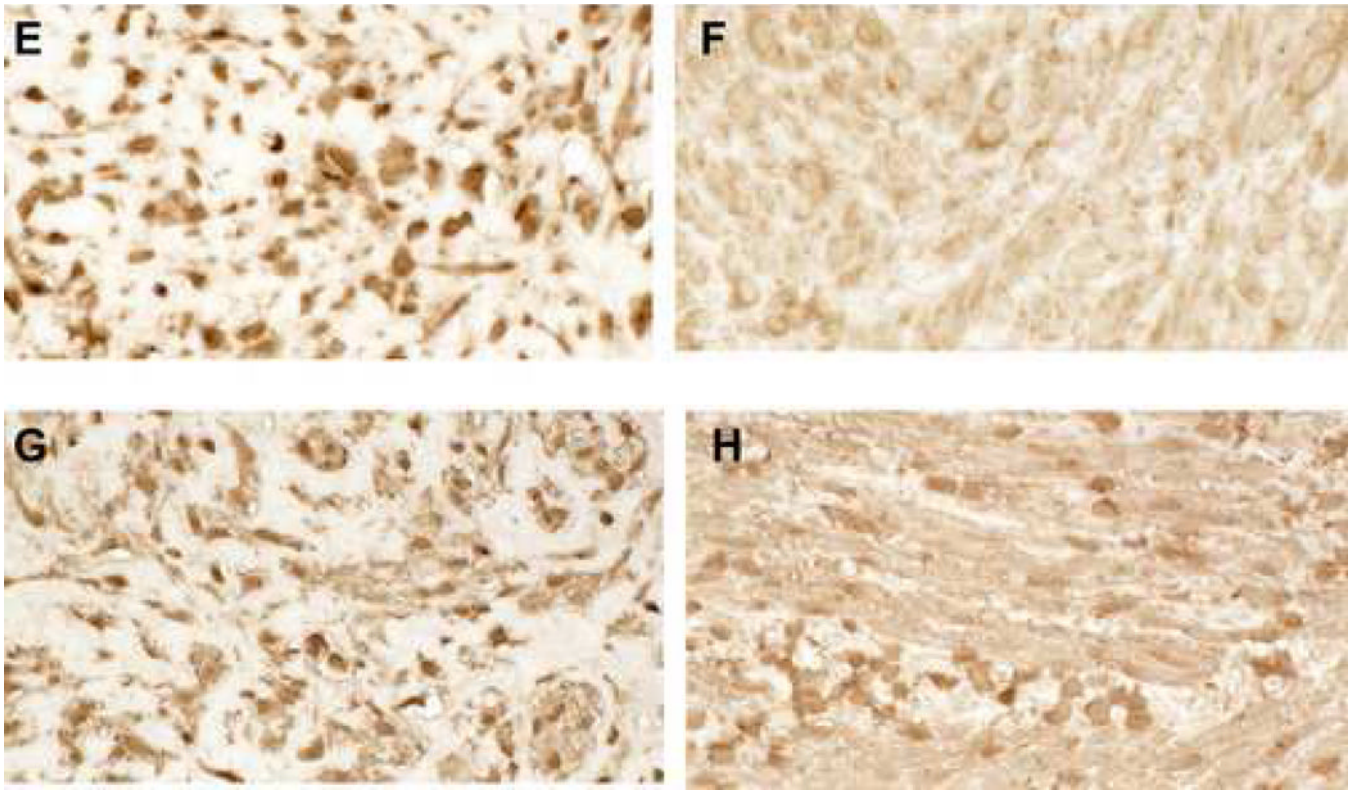

Figure 2. Structural changes associated with uterine leiomyoma

2A–D: FITC-Phalloidin staining of sections from matched leiomyoma and myometrial samples. Staining for actin in fibroid samples reveals a disordered structure and is markedly different from normal myometrium. Leiomyoma (A) and myometrium (B) were from the same uterus; leiomyoma (C) and myometrium (D) were from a separate specimen. Note the deformed nuclei and cell structure in A and C. Representative studies. Magnification 40X.

2 E,F: Staining of paired leiomyoma (E) and myometrium (F) for RhoA (1:1000) suggested increased staining. Magnification=40X.

2 G,H: Staining of paired leiomyoma (G) and myometrial (H) sections for alpha-smooth muscle actin (1:1500). Expression was slightly increased in leiomyoma cells. Magnification=40x

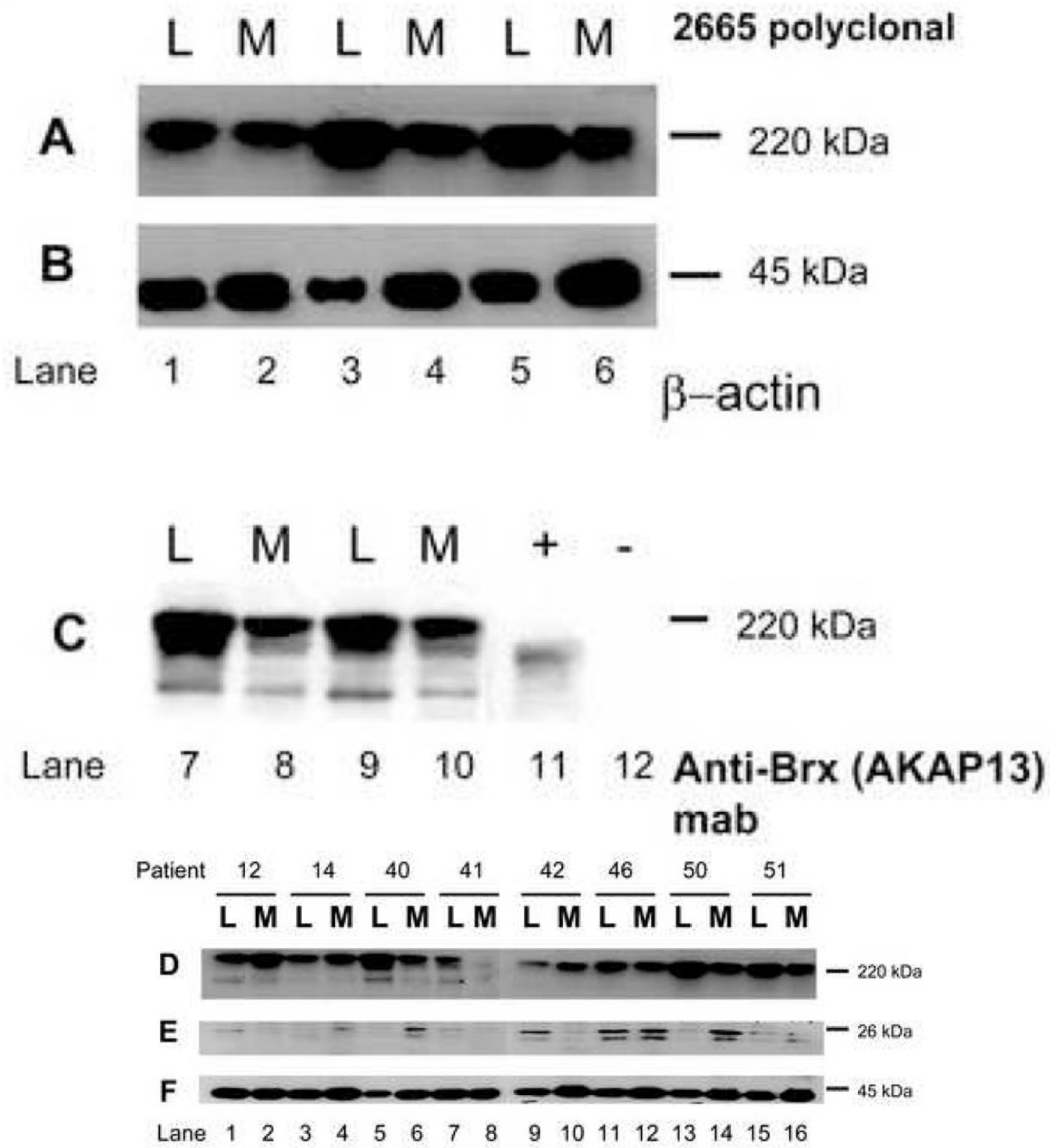

Figure 3. Altered expression of factors involved in mechanical transduction in matched surgical specimens of uterine leiomyoma and myometrium

3A: Western analysis of leiomyoma (L) and myometrial (M) lysates for expression of the Rho-GEF AKAP13 using 2665 affinity-purified antisera.29 A 220kDa band was present that was increased in leiomyoma compared to myometrium. Samples from patients 12–16, 40–41, 50, 51 were used for all western blots.

3B: Beta actin control for lysates in A.
3C: Western analysis for AKAP13 using monoclonal antibody directed against Brx (Upstate, Temecula, CA). A 220kDa band is identified. Positive control (+) consisted of lysates prepared from Cos-7 cells transfected with a construct expressing a 170kDa form of AKAP13. The negative control (−), lane 12, were lysates prepared from un-transfected Cos-7 cells (Cos-7 cells do not express AKAP13).
3D: Western analysis for AKAP13 in matched leiomyoma (L) and myometrial (M) lysates from 8 patients. In most, but not all pairs, expression of AKAP13 was greater in leiomyoma (L) compared to myometrium (M).
3E: Western analysis for RhoA in the same lysates. Readily extractable levels of RhoA were increased in some, but not all fibroid samples.
3F: Beta actin control for protein loading.

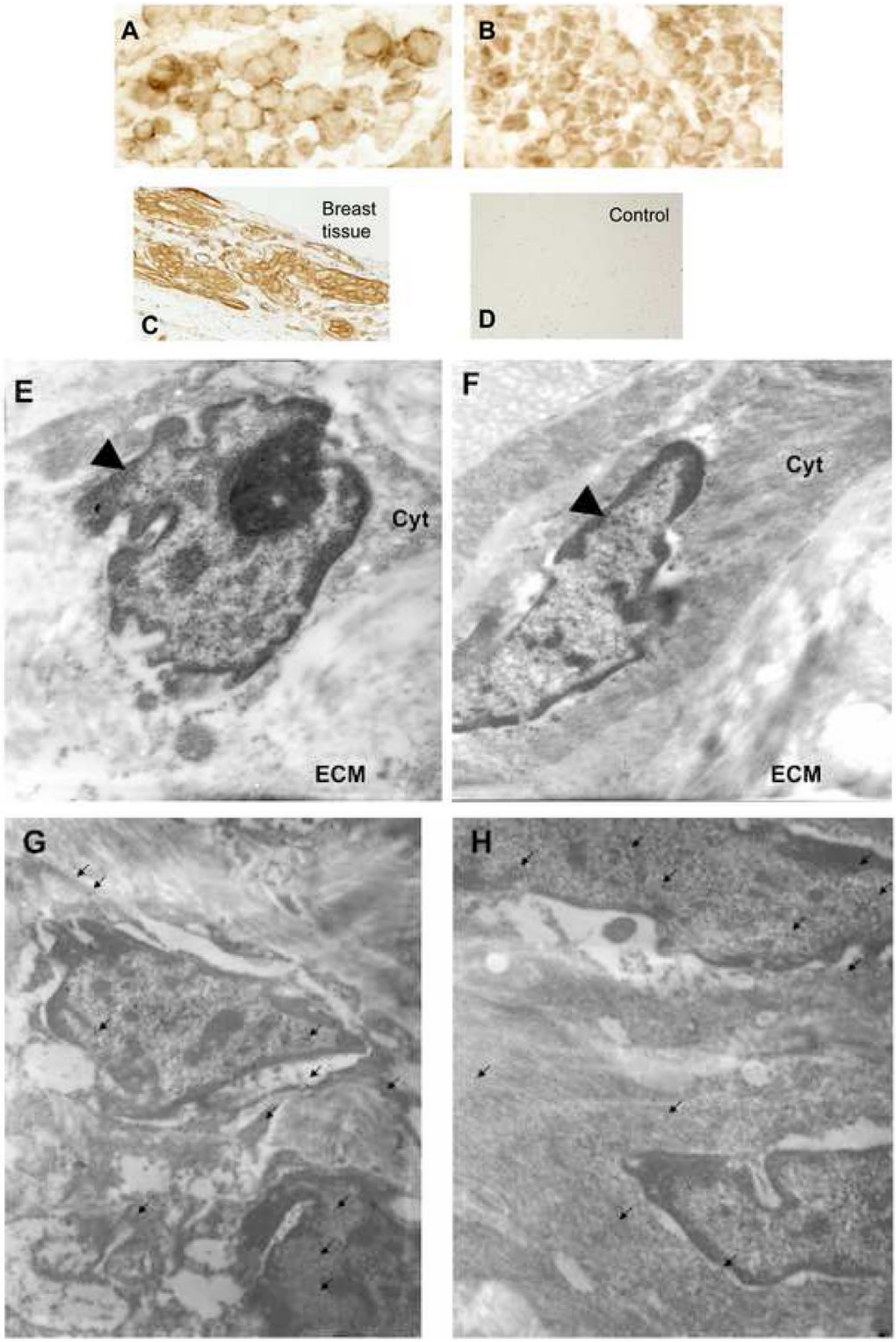

Figure 4. Subcellular distribution of AKAP13 in matched leiomyoma and myometrial specimens

4 A–D: Immunohistochemical localization of AKAP1 (1:500) in leiomyoma (A) and myometrium (B) tissues. Magnification=63X. Positive control, breast tissue (C); negative

control=fibroid tissue stained with pre-immune antisera (D). Staining for AKAP13 was often appeared increased with a peri-nuclear appearance in fibroids.

4 E, F: Immunogold study of matched leiomyoma (E) and myometrium (F) specimens using 2665 anti-sera directed against AKAP13. Note the angular cell shape, reduced cytoplasm, and notched nucleus in the leiomyoma (E) compared to myometrium (F). Round black dots indicate localization of protein. Black triangle points to nucleus. Cyt=cytoplasm; ECM=extracellular matrix. Magnification=21,000X. Samples from patients 18–21 were used for immunogold experiments.

4 G, H: Immunogold staining from another matched pair of leiomyoma (G) and myometrial (H) tissues stained with antisera directed against AKAP13. In this view, arrows point to AKAP13 expression in the nucleus, nuclear envelope and cytoplasm. Magnification=15,500X. Results were repeated in matched samples from 4 patients.

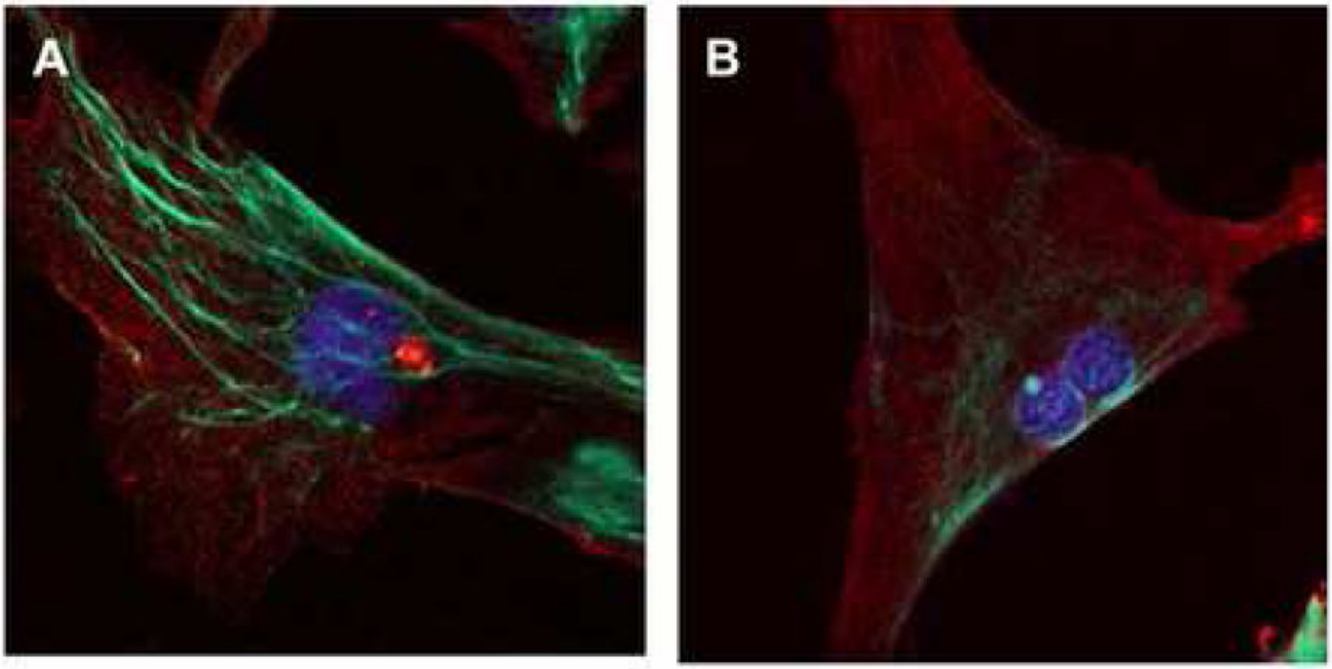

Figure 5. Altered focalization of AKAP13 to cytoskeletal structures in immortalized cultured leiomyoma and myometrial cell lines

5 A: Confocal laser microscopy of leiomyoma cell stained with antisera directed against AKAP13 (green) and alpha smooth muscle actin (red). AKAP13 protein is localized to cytoskeletal filaments. DAPI-stained nucleus appears blue.

5 B: Confocal laser microscopy of myometrial cell stained for AKAP13 (green) and alpha smooth muscle actin (red). Staining for AKAP13 protein is less robust. DAPI-stained nucleus appears blue. Results were repeated in 3 independent experiments.

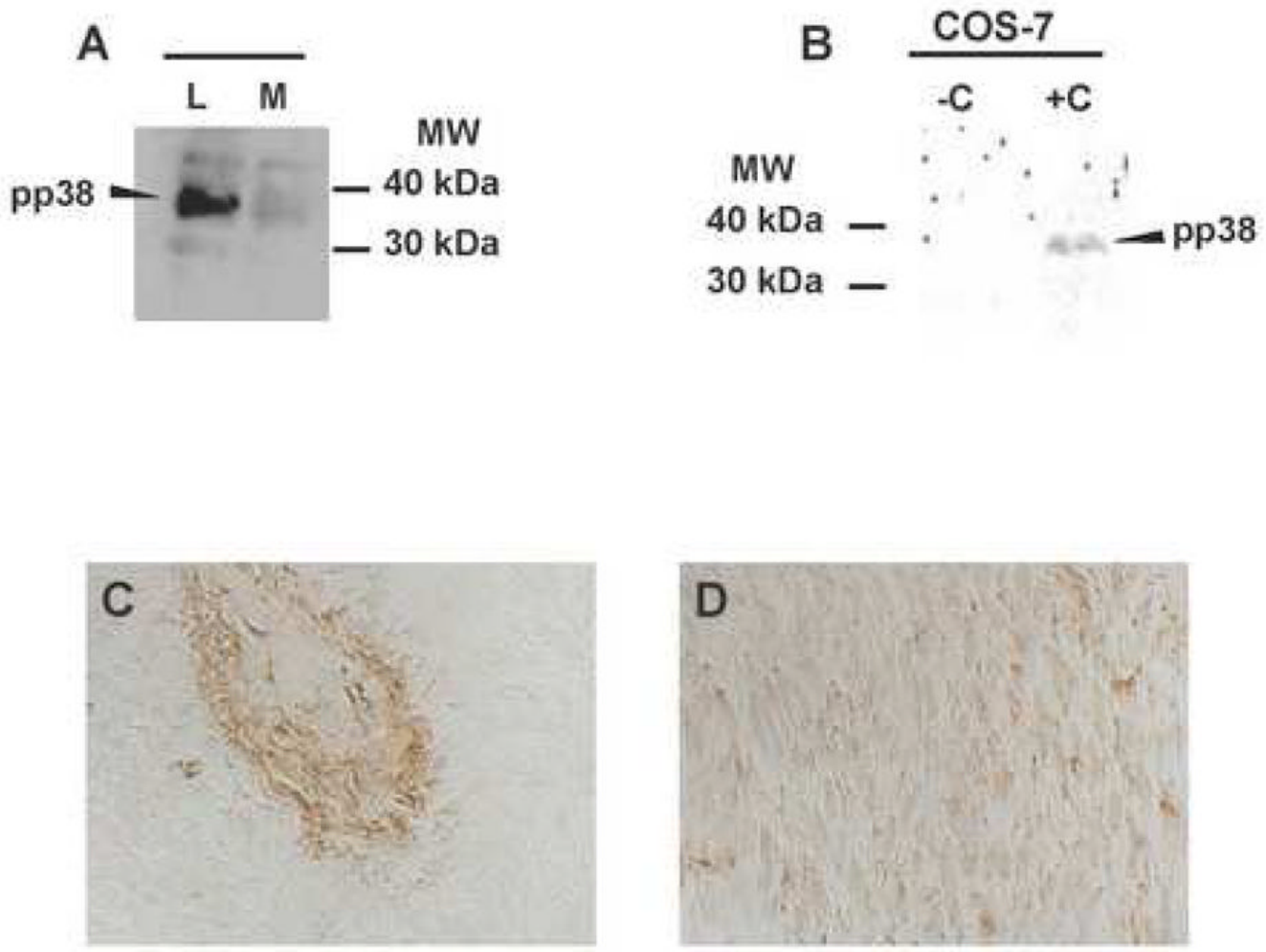

Figure 6. Evidence of activation of solid state signaling in leiomyoma cells

6A: Western analysis of phosphorylated p38MAPK in leiomyoma (L) and matched myometrial (M) samples. Findings were replicated in 3 experiments.

6 B: As a positive control for detection of phosphor-p38MAPK, lysates were prepared from Cos-7 cells were treated with anisomycin (+). Untreated Cos-7 cells served as a negative control.

6 C, D: Immunohistochemical staining of leiomyoma (C) or matched myometrial section (D) with antisera directed against phosphor-p38MAPK. Magnification=40X.

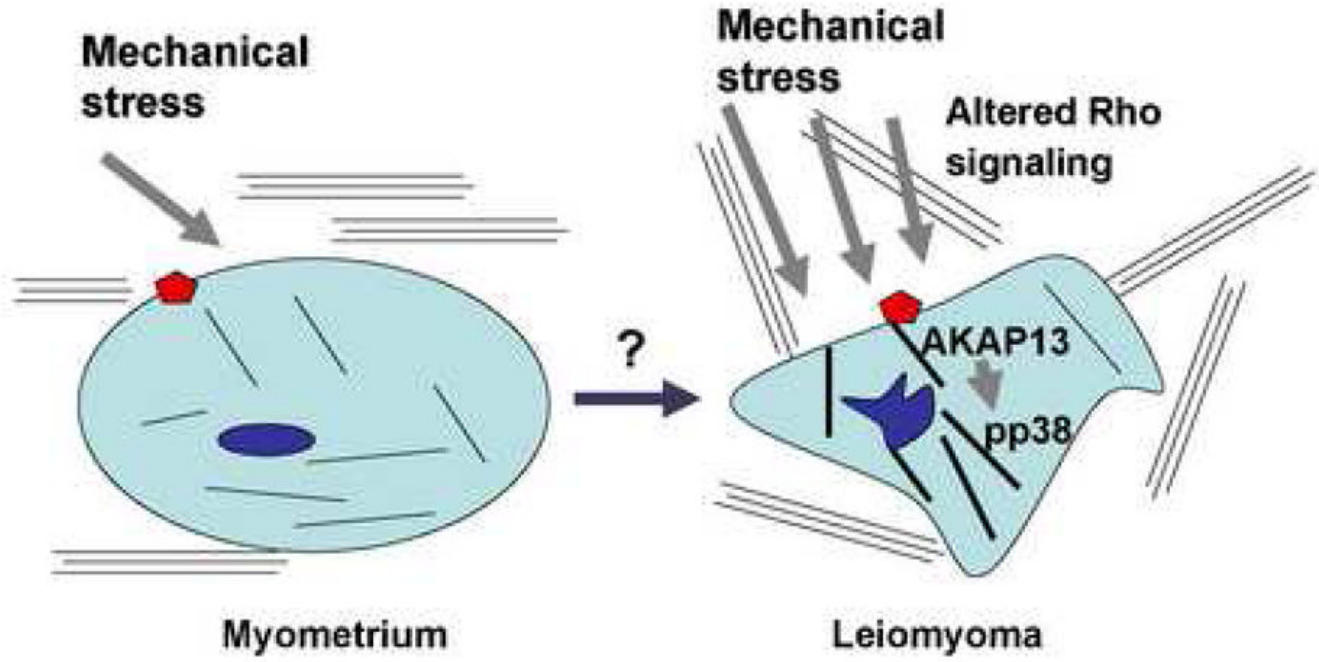

Figure 7. Model of altered mechanical stress in leiomyoma cells

Leiomyoma cells are under increased mechanical stress compared to myometrial cells. The extracellular matrix is abnormal in content and structure. Mechanical load is associated with alteration in actin organization as well as Rho-GEF expression (AKAP13). There is evidence for activation of stress-activated kinases, such as p38MAPK (pp38).

Table I

Patient characteristics

Patient #	Age	Race	Fibroid Size	Location	Time of Cycle
1	35	Caucasian	2×1.5×1.7	Submucosal	Follicular
2	39	African-american	7×7	Intramural	Periovulatory
3	37	Caucasian	5×4	Submucosal	Periovulatory
4	37	African-american	1.5×1.5×1.7	Intramural	Luteal
5	46	African-american	2×1.3×1.4	Submucosal	Follicular
12	39	African-American	1×1×1	intramural	luteal
14	37	white	5×4×4	intramural	ovulatory
16	37	African-American	1.5×12	intramural	anovulatory
18	38	African American	1.2×1.1×1.3	submucosal	follicular
19	47	Caucasian	3.5×3.5×3	subserosal	NA
20	47	African American	7×7×6	subserosal	NA
21	44	African American	4.2×4.5×5.5	intramural	NA
40	36	white	5.5×4×5	submucosal	ovulatory
41	49	Asian	7×5×8	subserosal	NA
42	46	white	5×5×5	intramural	luteal
46	46	African-American	4×4×4	subserosal	ovulatory
50	48	African-American	5×5×5	intramural	anovulatory
51	44	African-American	5×3×3	intramural	luteal

Am J Obstet Gynecol. Author manuscript; available in PMC 2009 June 15.

Table II

Microarray results for Stress-related Genes in leiomyoma and myometrium

Gene	L/M ratio
Alpha-cardiac actin	5.2
Alpha–smooth muscle actin	1.2
Alpha 1 actinin	−2.02
Alpha 1 actinin, skeletal muscle	−1.79
myosin	8.3
Tropomyosin 1 & 4	−3.6
Smooth muscle MHC	−3.3
Alpha-MHC consensus	2.37
Fibrillin 2	3
Vinculin	−1.15
Talin	1.39
ROCK (Rho-kinase)	−1
Rho-GEF FERM	−1.34
Rho-GEF 12	−1.06
Rho-GEF p115	1
Rho-GEF 4	1.2
Rho-GEF AKAP13	4
Endothelin receptor type B	−2.13
Endothelin receptor	−1.57

L/M, ratio of leiomyoma to myometrial signal

MHC, myosin heavy chain

GEF, guanine nucleotide exchange factor

Samples from patients 1–5 were used for microarray.